Optical quantum sensors for brain monitoring and imaging

Raffaele Di Vora

01.06.2022

UNIVERSITÀ DI SIENA 1240

Introduction

Brain monitoring: until recently, dominated by static neuroimaging

3 main traditional techniques:

- **electroencephalography (EEG)**: time resolution $\sim$ ms; spatial res. $\sim$ cm
- **magnetoencephalography (MEG)**: time resolution $\sim$ ms; spatial res. $\sim$ mm
- **functional magnetic resonance imaging (fMRI)**: time resolution up to $\sim$ 0.1 ms; spatial res. $\sim$ mm

  $\rightarrow$ better SNR due to blood oxygen level-dependent contrast technique, recently also from introduction of spin-relaxation free optical magnetometers

Limitation: large, expensive, patient has to stay still inside the scanner!!

Not wearable $\rightarrow$ spatial resolution limited by distance between sensor and brain

Optical techniques: promise to be more flexible

Optical techniques: general characteristics

Sensing principle: functional changes in tissue lead to changes in static neuroimaging

Main advantages over traditional techniques:

- smaller, typically more cost-effective
- wearable $\rightarrow$ adaptable to different environments $\rightarrow$ better suited to clinical applications
- Can exploit different wavelenghts to monitor various parameters in parallel

Disadvantage: strong scattering and absorption in human skull and scalp

$\rightarrow$ typical transmission for 7-11mm-thick skull: $\sim$ 2% @1064nm

$\rightarrow$ Some techniques only usable on soft tissues, brains of infants/small animal models

$\rightarrow$ difficult to use for morphological scanning

Optical techniques: overview /1

4 main techniques for label-free, non-invasive optical brain monitoring:

- **functional near-infrared spectroscopy (fNIRS)**: monitor cortical neural activity measuring dynamics of hemoglobin, but limited spatial resolution

- **diffuse correlations spectroscopy (DCS)**: measure blood flow thanks to scattering of photons by blood cells, but limited spatial resolution

- **photoacoustic imaging (PAI)**: high contrast and spatial resolution, limited by thick skill effect (ultrasound absorption $\sim$20 dB/cm)

- **optical coherence tomography (OCT)**: extremely accurate spatial information, good temporal resolution, extremely limited penetration depth

Consequence: only first two techniques usable for human brain monitoring!

Optical techniques: overview /2

Technology	Measurement Principle	Measuring Parameters	Wavelength (nm)	Source	Common Detector	penetration Depth	Spatial Resolution	Used as Wearable	Speed	Label Free	Cost
fNIRS	Scattering + absorption	$CMRO_2$, HbT	660–950	LED, LD, Laser	PD	A few cm	~1 cm/Fast	Yes	High	Yes	Low
DCS	Speckle fluctuation	BFI, $CMRO_2$	660–950	Laser (coherent)	APD	up to ~1.5 cm	~1 cm/ fast	Yes	High	Yes	Low
PAI	PA effect	$CMRO_2$, optical absorbers	500–1300	LD, Laser	PZT or array	up to 7 cm in soft tissues	Up to 1 µm	Yes	Depend on image size, Slow	Yes	High
OCT	Light coherence properties	CBF, $CMRO_2$	Visible +IR	Wide band source	PD	up to 2 mm	Up to 1 µm	No	Depend on image size, high	Yes	Low

$CMRO_2$ = cerebral metabolic rate of oxygen; HbT = concentration of hemoglobin; LD = laser diode; BFI = blood flow index; CBF = cerebral blood flow; PD = photodiode; APD = avalanche photodiode; PZT = piezoelectric transducer

functional Near-InfraRed Spectroscopy (fNIRS)

Sensing principle: wavelength-dependent absorption and scattering due to different energy level structure of functional molecules (e.g. hemoglobin)

Typically uses 2-3 wavelenghts in physiological window 650-950 nm $\rightarrow$ skin, tissues, bones $\sim$ transparent

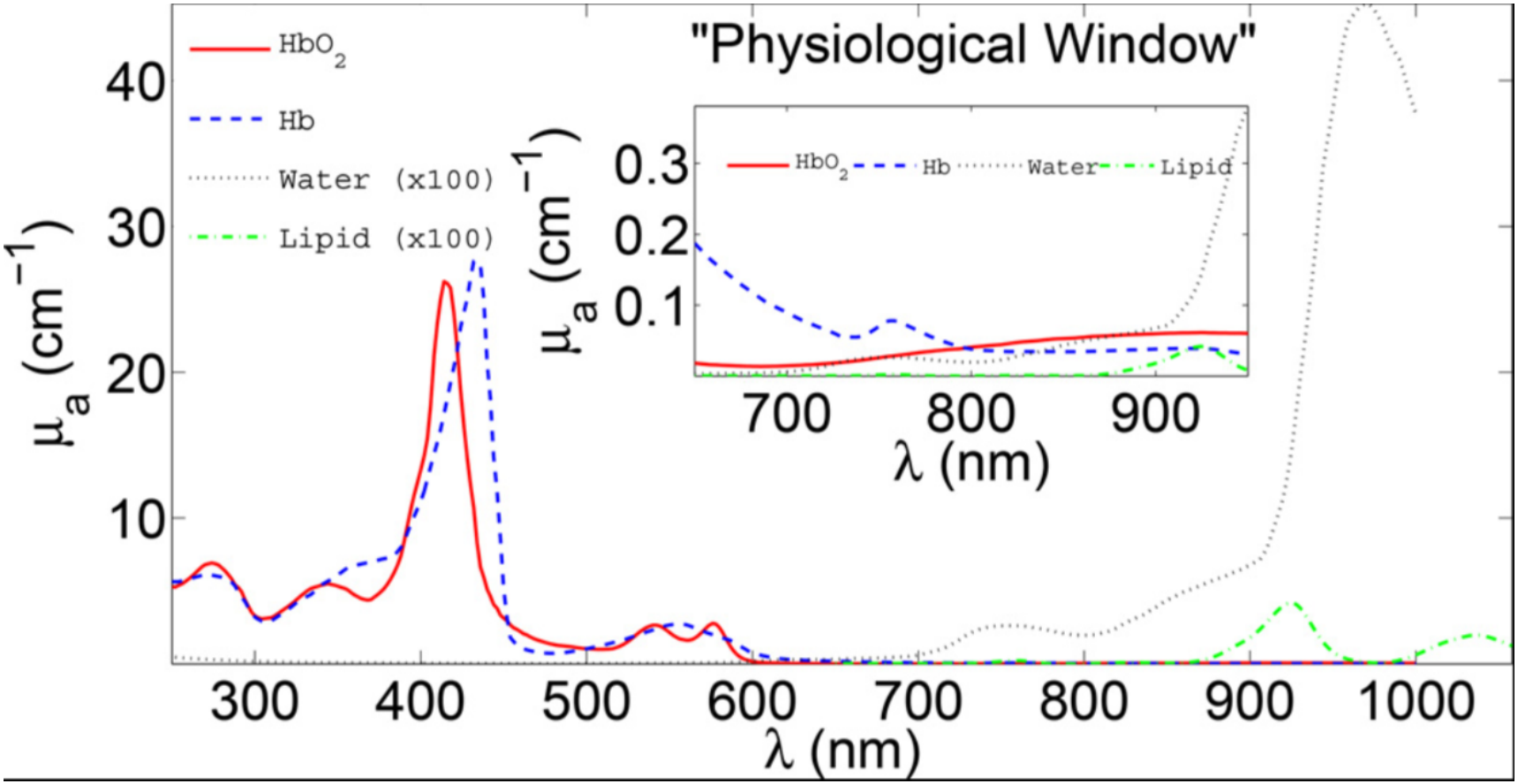

functional Near-Infrared Spectroscopy (fNIRS)

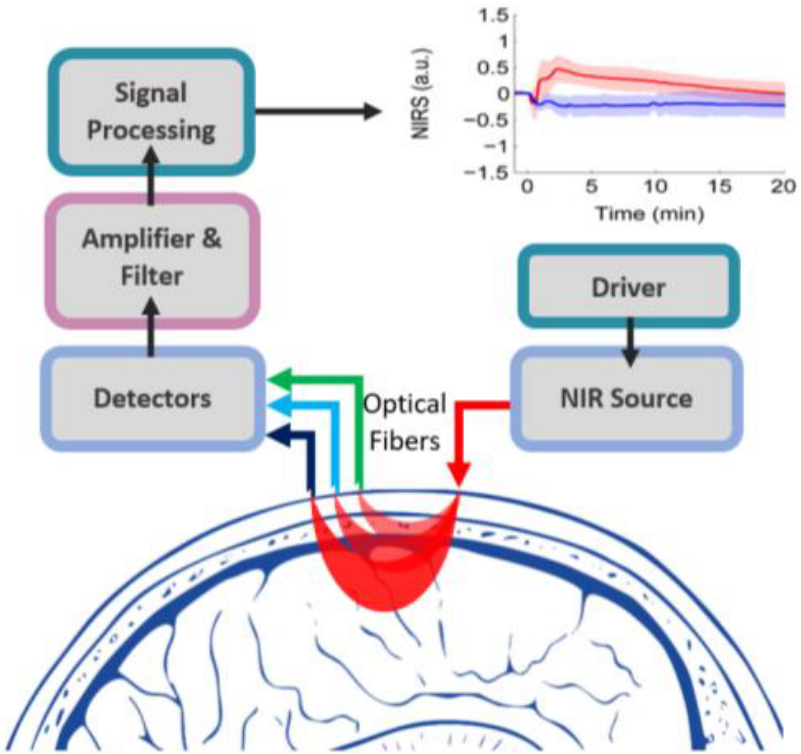

- Clinical applications:

preoperative localization of tumors/cancer therapy or neurodegenerative disease monitoring

mapping of functional areas before surgery

- Uses high-sensitivity photodiodes/photomultipliers to detect back-scattered light along "elliptical pathways"

$\rightarrow$ need for high-powered sources (LED, LD) near the brain

$$\mu(z) = \sum_{i=1}^{N} \mu_i(z) = \sum_{i=1}^{N} \sigma_i n_i(z)$$

$\mu(z)$ attenuation coefficient at point z, σ_i attenuation cross-section of species i, $n_i(z)$ number density of species i

$$T = e^{\int_0^d \mu(z)\, dz} = 10^{-A}$$

T transmittance coefficient, A absorbance coefficient, l optical path length

functional Near-Infrared Spectroscopy (fNIRS)

$$OD = log_{10}(\frac{I_0}{I_{in}}) = \mu_a \cdot [X] \cdot l \cdot DPF + G$$

OD optical density, I_0 measured light intensity, I_{in} incident light intensity, $[X]$ cromatophore concentration, DPF differential path length factor (determined through measurement of the mean time of flight of picosecond pulse or by frequency-domain NIRS at 4 different wavelengths), G geometrical parameter for the light's scattering properties (treated as constant)

By measuring the differentials in time, we obtain information on the changes in cromatophore concentrations:

$$\Delta[X] = \frac{\Delta OD}{\mu d}$$

(d total corrected photon path length)

$\rightarrow$ measuring at at least two wavelengths λ_1 and λ_2 (one below and one above the crossing point):

$$\begin{pmatrix} \Delta OD_{\lambda_1} \\ \Delta OD_{\lambda_2} \end{pmatrix} = \begin{bmatrix} \mu_{\lambda_1}^{Hb} d & \mu_{\lambda_1}^{HbO_2} d \\ \mu_{\lambda_2}^{Hb} d & \mu_{\lambda_2}^{HbO_2} d \end{bmatrix} \begin{pmatrix} \Delta[X]^{Hb} \\ \Delta[X]^{HbO_2} \end{pmatrix}$$

fNIRS - techniques /1

3 different fNIRS techniques:

- **Continuous Wave technique**
- **Frequency-Domain technique**
- **Time-Domain technique**

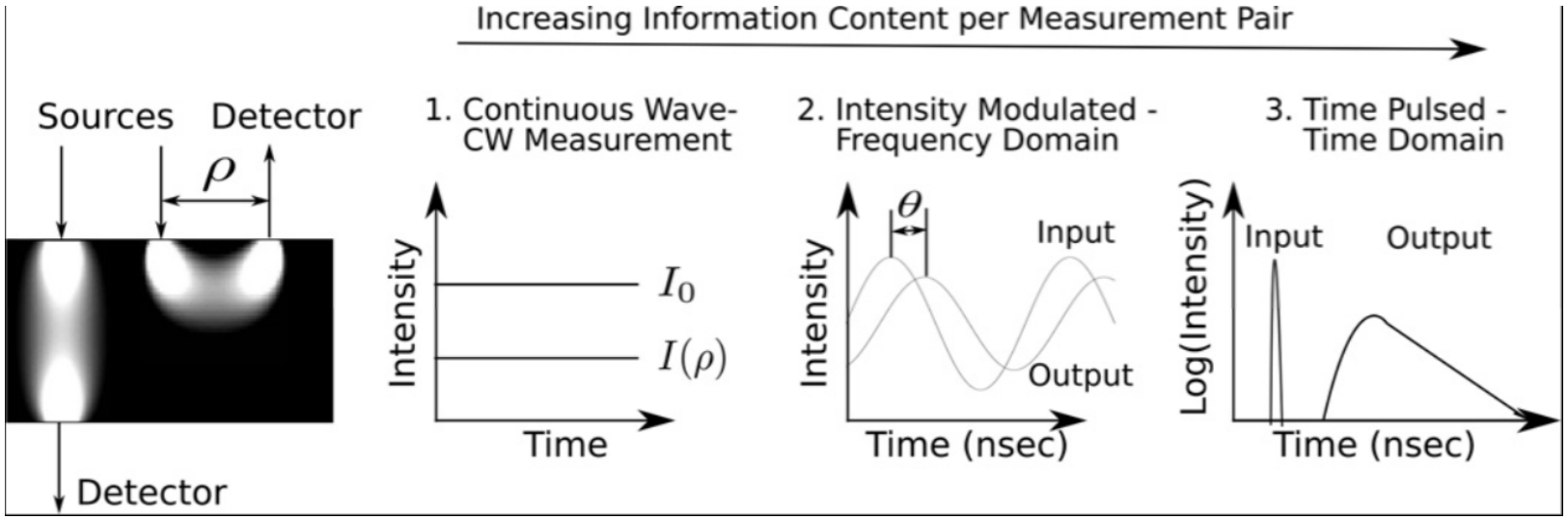

Absolute concentrations obtainable from total photon path length

fNIRS - techniques /2

- **Continuous Wave technique**

  low cost, miniaturized and wearable

  doesn't measure time-of-flight, so only monitors relative changes in the ratio HbO_2/Hb

  can't distinguish between absorption and scattering changes

  amplitude of different wavelengths modulated at kHz/10s of kHz frequency (i.e. using acousto-optic modulators) to distinguish them

  better SNR due to use of lock-in amplification

Lock-in amplification: If we multiply a periodic signal by a cosine/sine reference signal, the average amplitude is: $U_{out} = \frac{1}{2} V_{sign} \cdot cos\theta$

V_{sign} measured signal, θ dephasing btw reference and signal

$$\rightarrow \text{ using two detectors: } \begin{cases} X = \frac{1}{2} V_{sign} \cdot cos\theta \\ Y = \frac{1}{2} V_{sign} \cdot sin\theta \end{cases} \rightarrow \begin{cases} U_{out} = \sqrt{X^2 + Y^2} \\ \theta = arctan\frac{Y}{X} \end{cases}$$

fNIRS - techniques /3

Improvement due to lock-in amplification: because noise is wide-bandwidth
$P_{noise} = k_B \cdot T_{eff} \cdot \Delta\nu$, T_{eff} effective temperature of detection chain, $\Delta\nu$ measuring bandwidth
$\rightarrow$ measuring over small $\Delta\nu$, we improve SNR... but we also limit time resolution $\sim 1/\Delta\nu$

- **Frequency-Domain technique**

  intensity modulated CW laser, but at 10s/100s of MHz

  allows to measure attenuation, phase shift and average path length

  $\rightarrow$ allows to measure absolute values for Hb/HbO_2 due to estimation of reduced scattering coefficients

- **Time-Domain technique**

  uses very short ($\sim$ ps) near infrared laser pulses

  allows to obtain path length from time-of-flight $\rightarrow$ direct measure of scattering and attenuation $\rightarrow$ allows to measure absolute values for Hb/HbO_2

  more costly and bigger, but becoming smaller, more affordable and robust

  needs photon counters

Diffuse Correlations Spectroscopy (DCS)

Sensing principle: measure the Blood Flow Index (BFI) from optical properties of tissue (scattering from moving "speckles" i.e. blood cells)

Uses correlation diffusion equation (obtained from radiation transport equation + some approx.)

$\rightarrow$ allows to obtain hemodynamics from measurement of temporal autocorrelation function of the electric field $G_1(\tau)$

$G_1(\tau)$ related to fraction of moving scatterers over all scatterers α, to effective photon diffusion coefficient D_γ, to absorption and reduced scattering coefficients μ_a and μ_s'

$\rightarrow$ limited by estimation of μ_s', less sensitive to μ_a

Source: high coherence laser

Detectors: single-photon counting avalanche photodiodes + photon correlator

Clinical applications: high potential in cancer therapy monitoring (hemodynamics before/after)

Diffuse Correlations Spectroscopy (DCS)

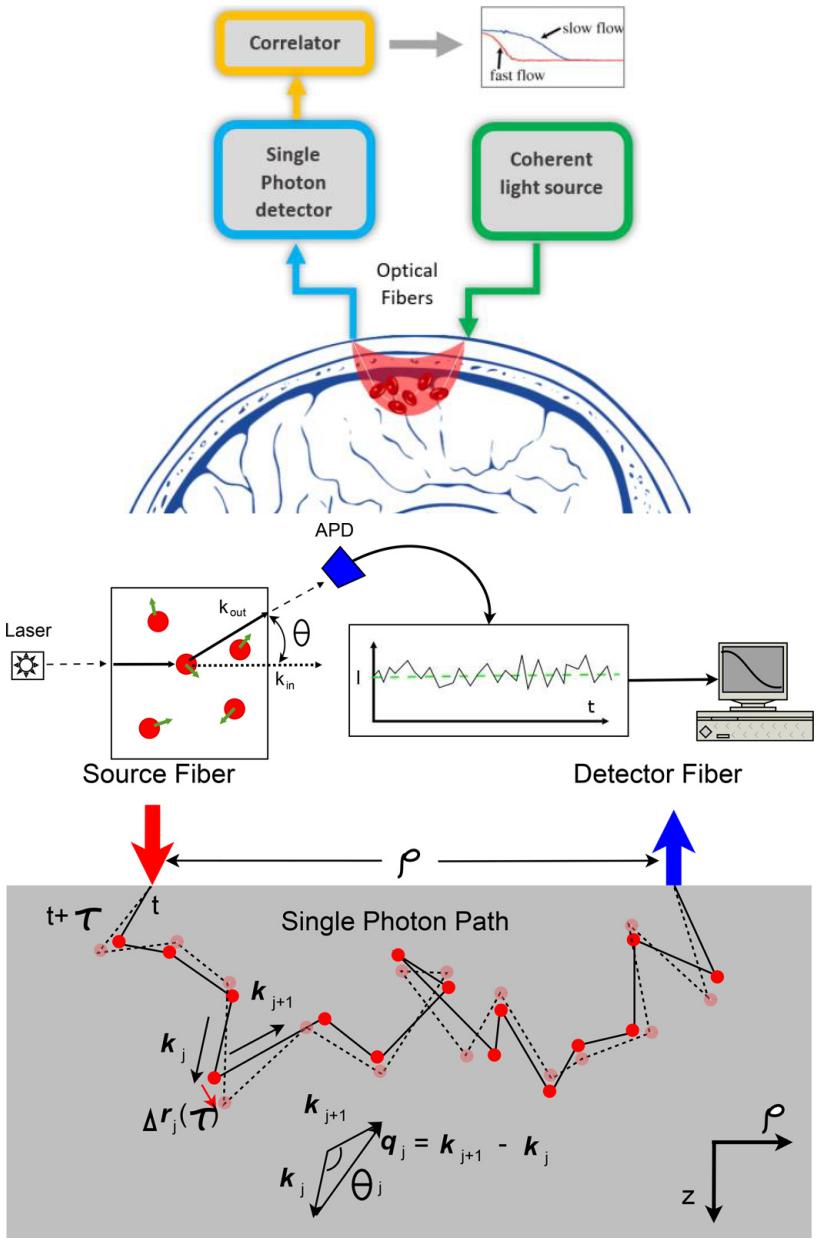

- Electric field and intensity autocorrelation functions:

$$A(\tau) = \int_{-\infty}^{\infty} E(t)E^*(t-\tau)\,dt$$

$$I(\tau) = \int_{-\infty}^{\infty} I(t)I(t-\tau)\,dt$$

$\rightarrow$ measure of normalized intensity autocorrelation

$$g_2(\tau) = \frac{\langle I(t)I(t-\tau)\rangle}{\langle I\rangle^2}$$

$\rightarrow$ then we obtain $g_1(\tau)$ from the Siegert relation:

$$G_2(\tau) = \langle I\rangle^2 + \beta|G_1(\tau)|^2$$

$$\rightarrow g_1(\tau) = \sqrt{g_2(\tau) - 1/\beta}$$

β constant dependent on number of speckles detected, coherence length and stability of the laser

Diffuse Correlations Spectroscopy (DCS)

- Correlation diffusion equation:

$$[D_\gamma \nabla^2 - v\mu_a - \tfrac{1}{3} v\mu_s' \, k_0^2 \langle \Delta r^2(\tau) \rangle] \, G_1(r,\tau) = -v \, S(r)$$

$\mu_s' = \mu_s(1 - \langle cos\theta \rangle) = 1/l^*$ reduced scattering coefficient (l^* reduced scattering length), $\mu_a = 1/l_a$ absorption coefficient (l_a absorption length), $D_\gamma = v/3\mu_s'$ photon diffusion coefficient, v speed of light in the medium, k_0 wave vector of light, r spatial position, $S(r)$ light source distribution

$\langle \Delta r^2(\tau) \rangle = \langle \Delta V^2 \rangle \tau^2$ for random flow with mean square velocity $\langle \Delta V^2 \rangle$

We can calculate the approximate impulse response:

for semi-infinite boundary conditions, the Green function is

$$G_1(r,\tau) = \frac{3\mu_s'}{4\pi} \left[\frac{e^{-K(\tau)\, r_1}}{r_1} - \left[\frac{e^{-K(\tau)\, r_b}}{r_b} \right] \right.$$

$$r_1 = \sqrt{1/\mu_s'^2 + r^2}; \; r_b = \sqrt{(2z_b + 1/\mu_s')^2 + 1/\mu_s'^2 + r^2}; \; K(\tau) = \sqrt{3\mu_a\mu_s' + 6\mu_s^2 \, k_0^2 \alpha \tau \, BFI}$$

Solve by fitting experimental points for μ_s', μ_a and BFI

$\rightarrow$ Additional constraint helpful! measure of $\mu_{eff} = \sqrt{3\mu_a\mu_s'}$ by pulsed fNIRS

DCS: iterative fitting

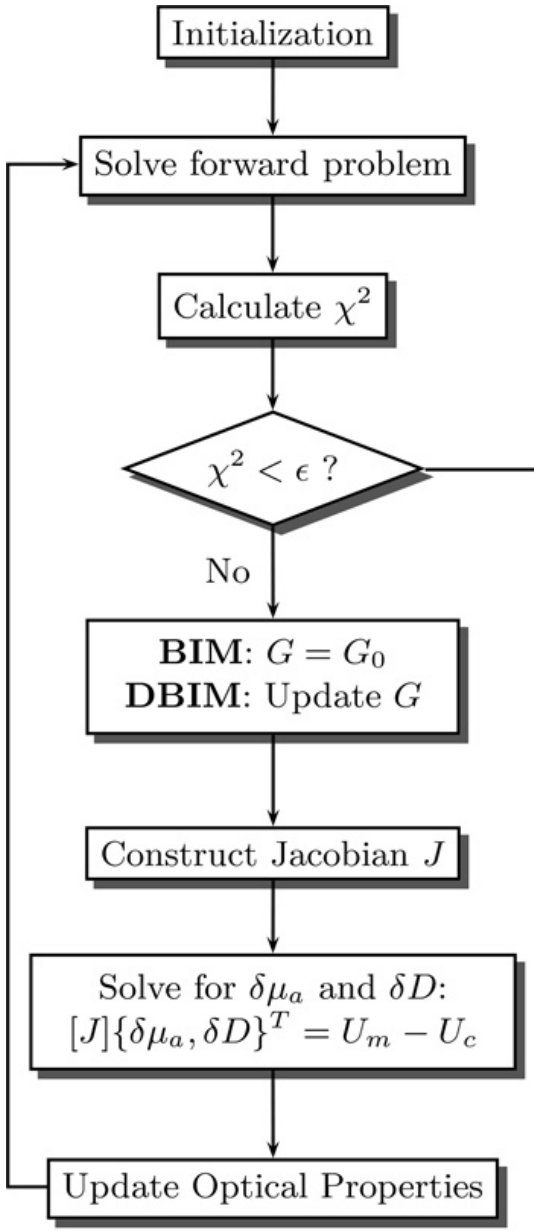

$$\mu_a(\mathbf{r}) = \mu_a^{(0)}(\mathbf{r}), D(\mathbf{r}) = D^{(0)}(\mathbf{r})$$

$$\nabla \cdot \left(D^{(k)}(\mathbf{r})\nabla U_c(\mathbf{r}, \mathbf{r_s})\right) - \left(v\mu_a^{(k)}(\mathbf{r}) + i\omega\right) U_c(\mathbf{r}, \mathbf{r_s}) = -vS(\mathbf{r}, \mathbf{r_s})$$

$$\chi^2 = \sum_{i=1}^{NM} \left| \frac{U_m(\mathbf{r_d}, \mathbf{r_s})_i - U_c(\mathbf{r_d}, \mathbf{r_s})_i}{\sigma_i} \right|^2$$

BIM: Born Iterative Method
DBIM: Distorted Born Iterative Method

$$\nabla \cdot \left(D^{(k)}(\mathbf{r})\nabla G(\mathbf{r_d}, \mathbf{r})\right) - \left(v\mu_a^{(k)}(\mathbf{r}) + i\omega\right) G(\mathbf{r_d}, \mathbf{r}) = \delta(\mathbf{r_d} - \mathbf{r})$$

$$[J] = \left[\frac{\partial U_c}{\partial \mu_a}, \frac{\partial U_c}{\partial D}\right]$$

SVD, ART, SIRT, CGM, etc.

$$\mu_a^{(k+1)}(\mathbf{r}) = \mu_a^{(k)}(\mathbf{r}) + \delta\mu_a(\mathbf{r}),$$
$$D^{(k+1)}(\mathbf{r}) = D^{(k)}(\mathbf{r}) + \delta D(\mathbf{r})$$

fNIRS: finger tapping demonstration

One sensor positioned on contralateral sensorimotor cortex, one on area unrelated to movement planning and execution; subject told to finger tap between vertical bars in graphs

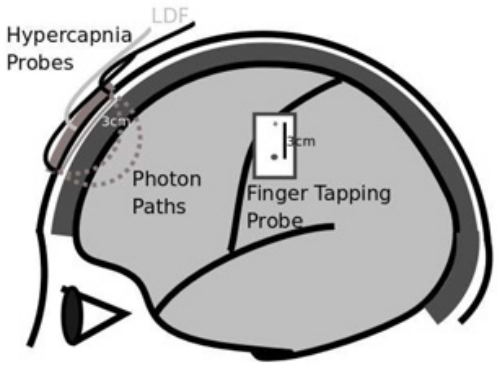

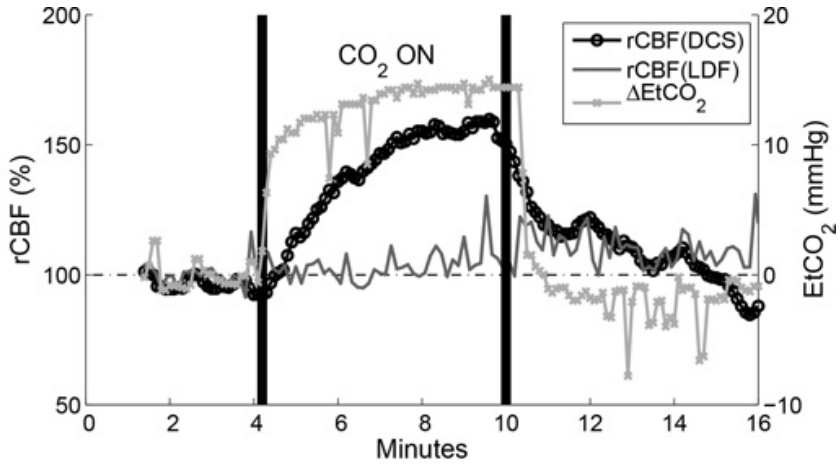

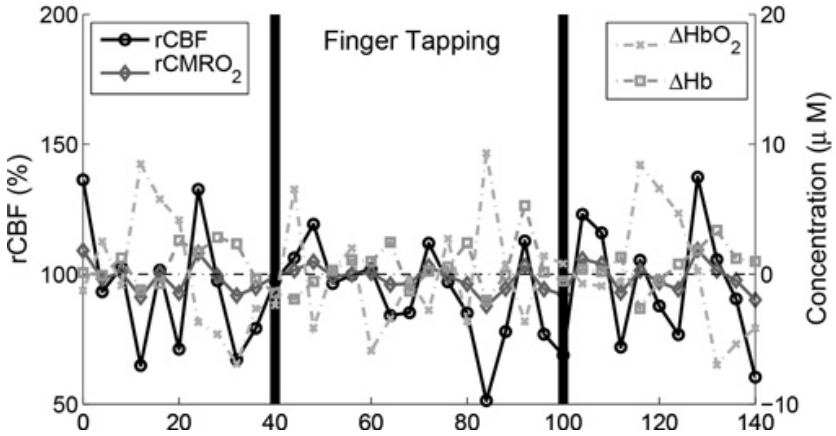

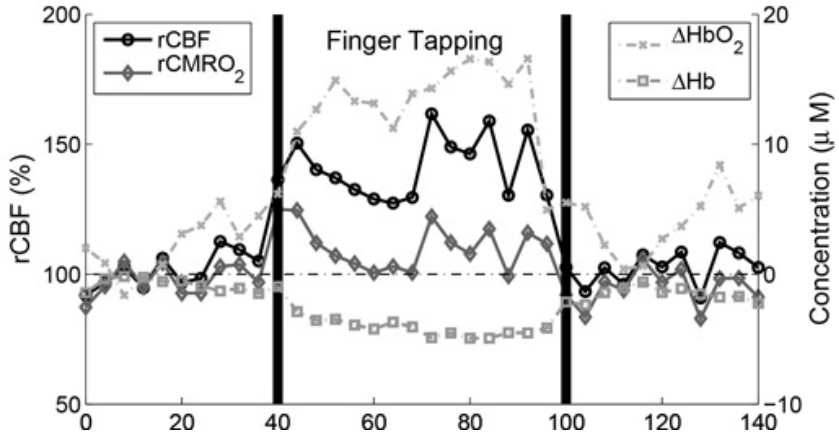

DCS: models and measures of $g_1(\tau)$

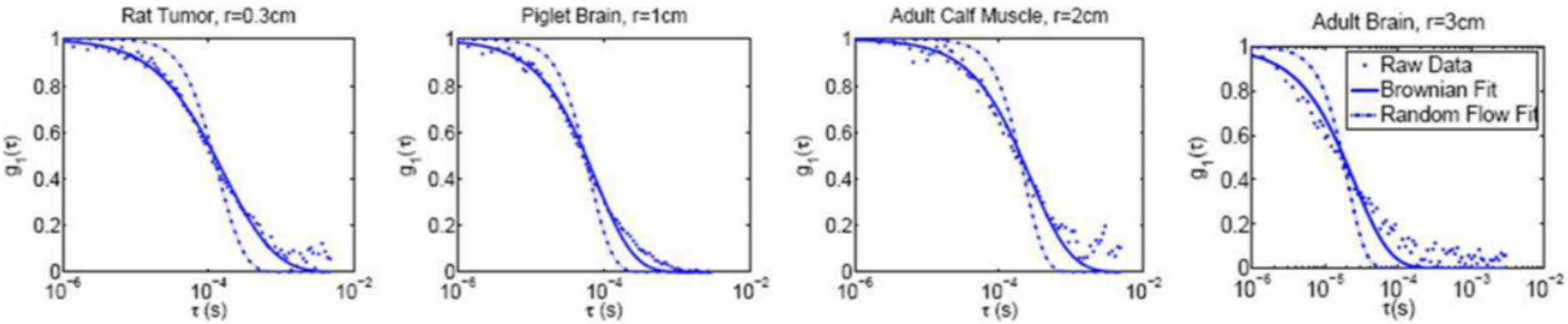

Measure of blood flow in rat when flow ensured by heart/by heart pump; same measure for rat alive/dead

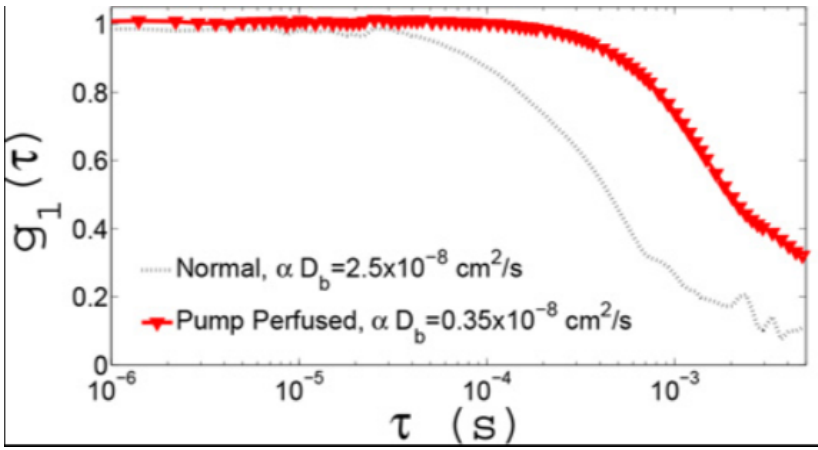

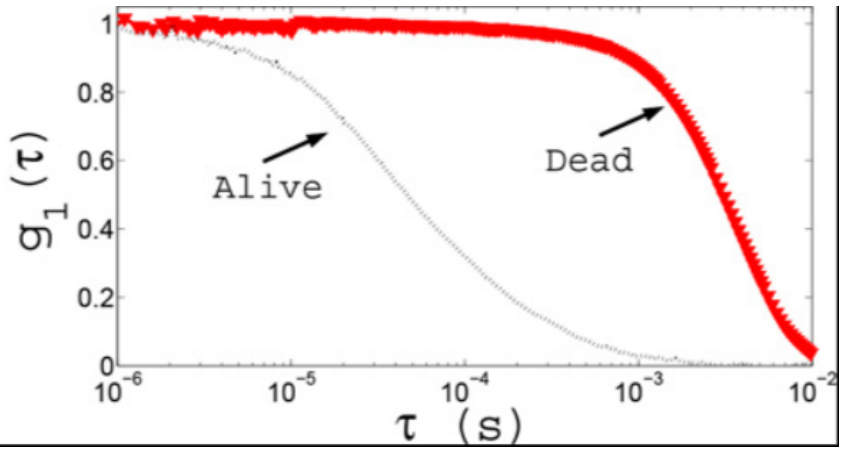

Basic experimental schemes of PAI and OCT

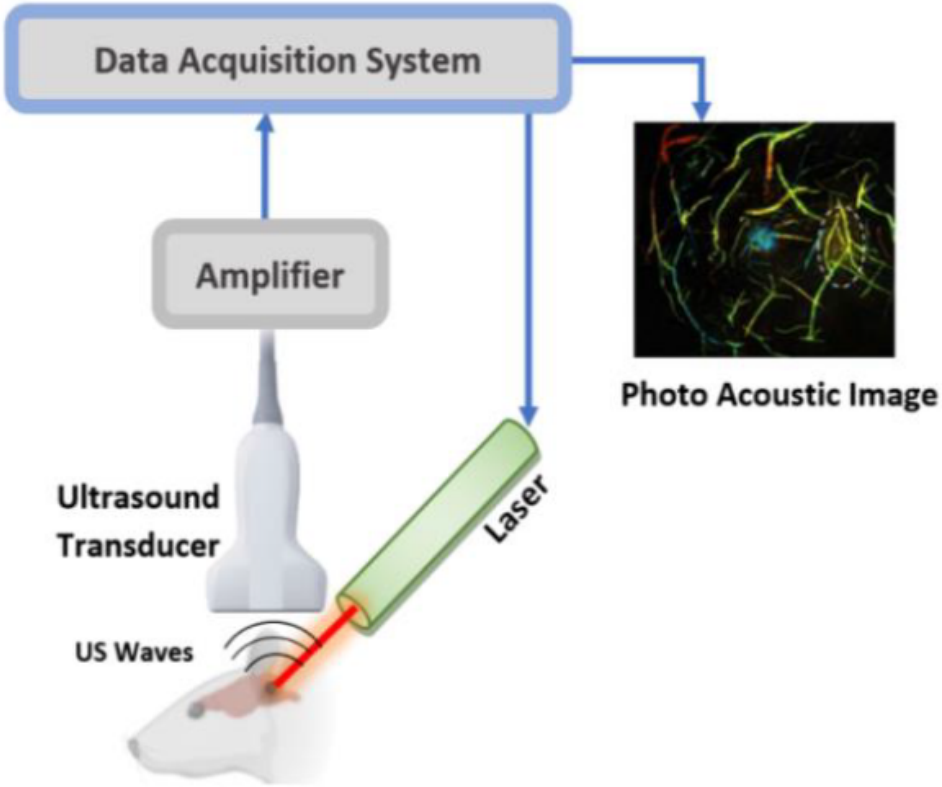

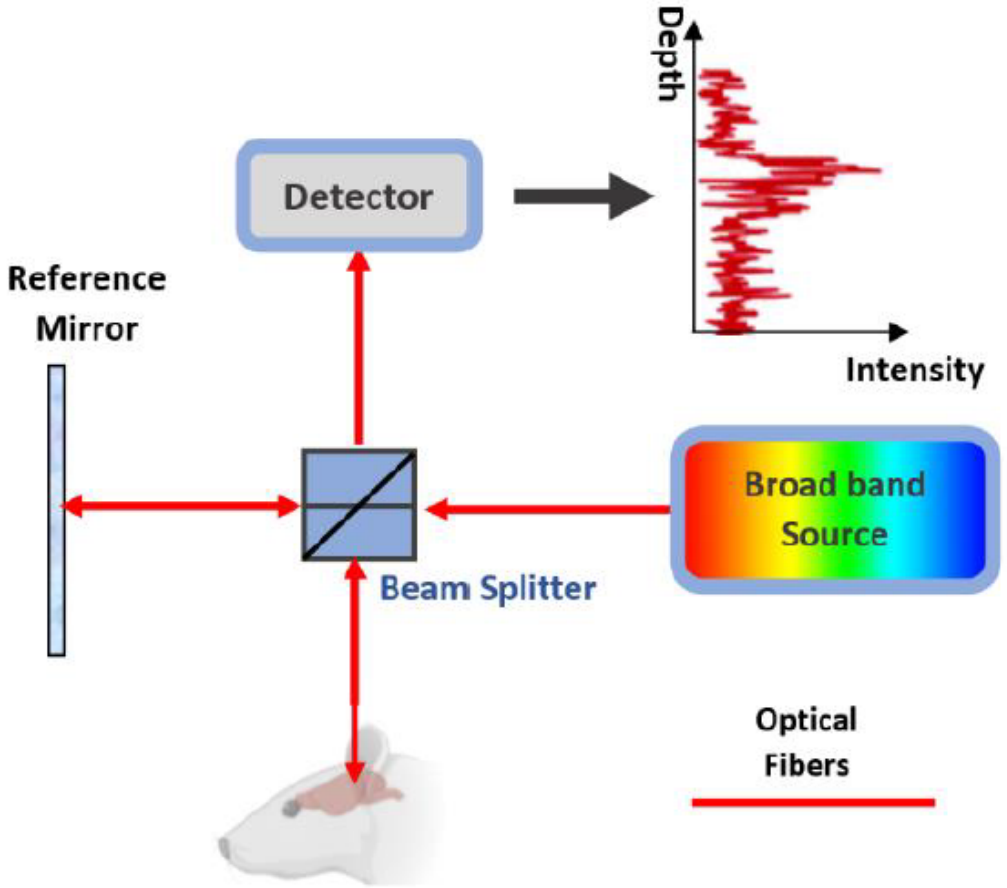

Bibliography

- "Optics Based Label-Free Techniques and Applications In Brain Monitoring" - Priya Karthikeyan, Sadegh Moradi, Hany Ferdinando, Zuomin Zhao and Teemu Myllylä; https://doi.org/10.3390/app10062196 (2020)

- "Differential Path-Length Factor's Effect on the Characterization of Brain's Hemodynamic Response Function: A Functional Near-Infrared Study" - Muhammad A. Kamran, Malik M. N. Mannann and Myung Yung Jeong; https://doi.org/10.3389/fninf.2018.00037 (2018)

- "Diffuse correlation spectroscopy for measurement of cerebral blood flow: future prospects" - Erin M. Buckley, Ashwin B. Parthasarathy, P. Ellen Grant, Arjun G. Yodh, Maria Angela Franceschini; DOI: 10.1117/1.NPh.1.1.011009 (2014)

- "Diffuse Optics for Tissue Monitoring and Tomography" - T. Durduran, R. Choe, W. B. Baker, A. G. Yodh; DOI: 10.1088/0034-4885/73/7/076701 (2010)

- "Chapter 4 Correlation Diffusion 4.1 Introduction" - Harvard lecture notes; https://www.nmr.mgh.harvard.edu/PMI/PDF/boas-diss/ch4.pdf

Thank you for your attention!!